ENCIT 2018

ABCM Associação Brasileira de Engenharia e Ciências Mecânicas

17th Brazilian Congress of Thermal Sciences and Engineering
November 25th-28th, 2018, Águas de Lindóia, SP, Brazil

ENCIT-2018-0381
COMPUTATIONAL SIMULATION OF TAYLOR BUBBLES MOTION IN A STAGNANT LIQUID INSIDE A VERTICAL COLUMN

Francisco R. T. do Nascimento
Marcos B. de Azevedo
José L. H. Faccini
Maria L. Moreira
Instituto de Engenharia Nuclear (IEN/CNEN), Rua Hélio de Almeida 75 - Cidade Universitária - Ilha do Fundão - CEP 21941-906 - Rio de Janeiro - RJ - Brasil.
rogerio.tdn@gmail.com; bertrand@ien.gov.br; faccini@ien.gov.br; malu@ien.gov.br.

Jian Su
Programa de Engenharia Nuclear, PEN/COPPE-UFRJ, Av. Horácio Macedo, 2030, Bloco G - Sala 206 - Centro de Tecnologia, Cidade Universitária, Ilha do Fundão, 21941-914 - Rio de Janeiro, RJ - Brasil.
sujian@nuclear.ufrj.br

Abstract. *In the present work, the motion of single Taylor bubbles in a vertical column of stagnant liquid was computationally simulated by using the open source software Open FOAM. The simulated column consists of a tube with 2 m in length and inner diameter of 0.024 m, sealed at the ends and partially filled with water. Experiments were also performed under these conditions in order to measure some bubble parameters. The computational simulation was performed solving a mathematical model formed by the isothermal, incompressible and laminar Navier-Stokes equations. In addition, it was assumed that the fluids are immiscible and no turbulence models were used. The equations were discretized by the VOF (volume of fluid) method, and solved using the Gauss iteration method. Numerical solutions were obtained for the bubble velocities and profiles which were compared with the experimental results and correlations from literature.*

Keywords: *Computational simulation; Taylor bubbles; Open FOAM; Stagnant liquid column; Vertical flow.*

1. INTRODUCTION

Multiphase flows find the most diverse range of applications in various areas of knowledge. More specifically in nuclear industry a phenomenon of considerable interest that involves these flows, is the nucleate boiling, which is responsible for the appearance of bubbles in the outer wall of the fuel rods present in the reactor core. The control of such phenomena is fundamental for the preservation of the integrity of the fuel elements as well as the safe operation of the nuclear plant.

Another phenomenon associated with the cooling processes of the primary system of a nuclear plant is called slug flow (Ghajar, 2005). Slug flow is one of the common flow patterns in gas-liquid flow and is accompanied by fluctuations in pipe temperature. High pipe wall temperatures result in "dryout", which may cause damages in the nuclear power generating systems. Long bullet-shaped bubbles, also called Taylor bubbles, which occupy nearly the entire cross-section of the pipe, and a liquid slug between successive bubbles characterize the slug flow. The liquid moves around the bubbles in a thin film and expands at the rear of the bubble, inducing a liquid wake (Fig.1).

Dumitrescu (1943) performed the first relevant study concerning individual bubbles rising in stagnant liquids. He derived a Taylor bubble profile for air-water systems from potential flow and proposed a correlation to estimate the bubble velocity U_0. Dumitrescu's shape profile was divided into two regions, the nose region and the film region (Nogueira *et al.*, 2006):

For $\frac{Z}{D} \leq 0.25$,

$$\frac{Z}{D} = 0.375 \left[1 - \sqrt{1 - 7.112 \left(\frac{r}{D} \right)^2} \right]; \tag{1}$$

For $\frac{Z}{D} \geq 0.25$,

$$\frac{Z}{D} = \frac{0.0615}{\left(1 - 4 \left(\frac{r}{D} \right)^2 \right)^2}. \tag{2}$$

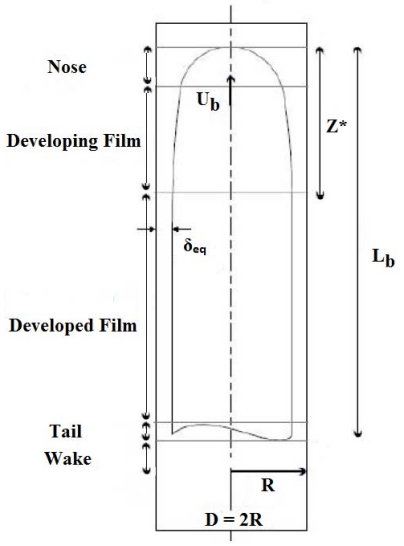

Figure 1. Schematic of a Taylor bubble rising in a vertical stagnant water column.

In Eqs. (1) and (2), Z is the axial distance from the tip of the bubble nose, r is the radial distance from the tube axis and D is the inner tube diameter.

From the experimental point of view, a pioneering work is attributed to Davies and Taylor (1950), who carried out experiments using both water and nitrobenzene, and studies were done on velocity, surface tension, bubble profile, among others. Nogueira *et al.* (2006) performed measurements by using the particle image velocimetry (PIV) and pulsed shadowgraphy techniques (PST) on bubbles generated from an air injection device in a co-current liquid column. In this work the measures related to bubble velocity are based on the expression attributed to Nicklin *et al.* (1962):

$$U_b = cU_L + \alpha\sqrt{gD} = cU_L + U_0, \tag{3}$$

where, U_b is the bubble velocity, c and α are constants, U_L is the liquid velocity, U_0 is the velocity of the bubble rising in stagnant liquid and g is the gravity acceleration. For low viscosity liquids, the expression $U_0 = 0.35\sqrt{gD}$ is in agreement with the works of Dumitrescu (1943) and of Davies and Taylor (1950). In addition, Nicklin *et al.* (1962) proposed relations for the study of liquid film thickness.

Despite the advances of commercial codes and computers in general, the computational simulation of multiphase flows is still not a simple task (Hiltunen *et al.*, 2009). For a gas-liquid two-phase flow, the main difficulty which distinguishes from single phase flows is the existence of deformable interfaces. Lagrangian and Eulerian strategies have been employed in the last years in order to develop a wide range of methods for advecting a sharp interface (Tryggvason *et al.*, 2011). Nowadays, most CFD codes use variants of the volume-of-fluid (VOF) method for the interface advection step in their interfacial flow solvers. The VOF method (Hirt and Nichols, 1981) can track the motion of gas-liquid boundary using a transport equation for volume fraction occupied by each phase, which is appropriate for the simulation involving two immiscible fluids, and can be used to accurately predict the profile of the interface between the fluids (Zheng *et al.*, 2007).

Roenby *et al.* (2016) devised a numerical method, called IsoAdvector, for passive advection of a surface, such as the interface between two incompressible fluids, across a computational mesh. It was developed for general meshes consisting of arbitrary polyhedral cells. The algorithm is based on the VOF idea of calculating the volume of one of the fluids transported across the mesh faces during a time step. Initially, an isosurface concept was exploited for modeling the interface inside cells in a geometric surface reconstruction step. Then, from the reconstructed surface, the motion of the face-interface intersection line was modeled for a general polygonal face in order to obtain the time evolution within a time step of the submerged face area. Integrating this submerged area over the time step leads to an accurate estimate for the total volume of fluid transported across the face. The IsoAdvector algorithm intends to work on arbitrary meshes, retaining the accuracy of the geometric schemes by explicitly approximating the interface, and yet keep the geometric operations at a minimum in order to obtain acceptable calculation times.

In the present work, a computational simulation of the motion of single Taylor bubbles in a vertical stagnant liquid column was performed in the open source software Open FOAM using the InterFlow solver and the IsoAdvector method, in order to test them in simulations of bubbles with this geometry. Numerical solutions were obtained for the bubble velocities and bubble profiles, which were compared with experimental results and correlations from literature.

2. EXPERIMENTAL EQUIPMENT

The experimental data were obtained from vertical columns partially filled with stagnant liquid. The columns consisted of acrylic tubes with 2.0 m in length and inner diameter 0.024 m sealed at the ends. A Taylor bubble with length L_b was formed by the inversion (t_1 to t_2) of the tube partially filled with distilled water to leave an air pocket of length L_0 (Fig.2).

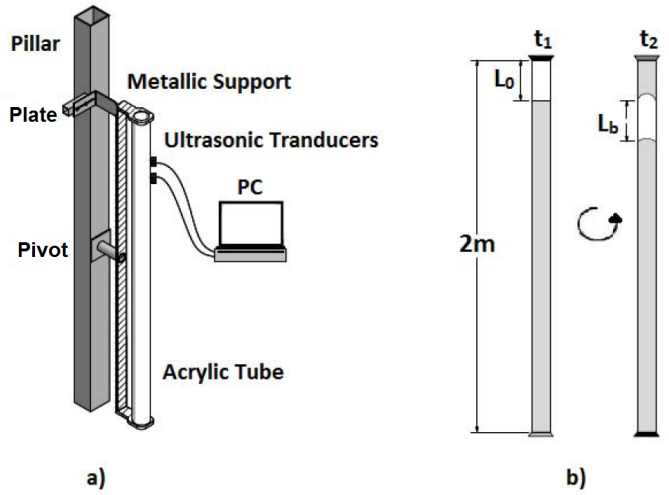

Figure 2. Schematic of the Test Section.

The velocities and profiles of the Taylor bubbles were determined by using a pulse-echo ultrasonic technique. Details about the experimental procedures can be found in De Azevedo *et al.* (2017).

3. MATHEMATICAL FORMULATION

3.1 Governing Equations

The mathematical is formed by the well known conservation equations of mass and momentum, respectively, applied in both gas and liquid phase:

$$\frac{\partial \rho}{\partial t} + \nabla.(\rho u) = 0; \tag{4}$$

$$\frac{\partial \rho u}{\partial t} + \nabla.(\rho u u) = -\nabla.p + \nabla T + \rho f + f\sigma, \tag{5}$$

where ρ is the fluid density (kg/m^3), u is the velocity vector (m/s), p is the pressure (Pa), T is the stress tensor, f represents the body forces and $f\sigma$ is the surface tension. To solve the mass and momentum conservation equations, it was used a laminar flow model, where a laminar flow and a Newtonian incompressible fluid is assumed.

The VOF method adds one governing equation (the advection equation) for the transport of the volume fraction α:

$$\frac{\partial \alpha}{\partial t} + \nabla.(\alpha u) = 0, \tag{6}$$

where, $\alpha = 1$ corresponds to a control volume entirely occupied by water and $\alpha = 0$ corresponds to a control volume containing only air. The value of α is averaged in each of the mesh cells. The interface between the phases is found in cells where $0 < \alpha < 1$. The second term in Eq. (6) is referred to as the advection term (Olsson, 2017).

In the VOF method, it is difficult to properly represent the value transitions at the interface between two phases, which can be overcome by the use of additional surface capture methods. In recent versions of OpenFOAM, a newly developed method (IsoAdvector) was introduced together with a solver named Interflow, which is an improvement of the InterFOAM solver.

3.2 The Interflow Solver

The Interflow solver uses a scheme named MULES for improving the surface sharpness. MULES is a numerical scheme where the advection term in Eq.(6) is modified to compress the surface (Olsson, 2017). The scheme is obtained

by firstly rewriting the advection equation to integral form:

$$\int_{\Omega_i} \frac{\partial \alpha}{\partial t} dV + \int_{\partial \Omega_i} \alpha u.ndS = 0, \tag{7}$$

where Ω_i represents each cell, $\partial \Omega_i$ is the cell boundary and n is the cell boundary normal.

The equation is then discretized, using any time-stepping scheme for the first term and writing the second term as a sum over each face of the cell:

$$\frac{\alpha_i^{n+1} - \alpha_i^n}{\partial t} = -\frac{1}{|\Omega_i|} \sum_{f \in \partial \Omega_i} \left(F_u + \lambda_M F_c\right)^n, \tag{8}$$

where F_u and F_c are the advective fluxes and λ_M is a delimiter taking the value 1 at the surface and 0 elsewhere.

3.3 The IsoAdvector Method

The IsoAdvector method uses the concept of isosurfaces to calculate more accurate face fluxes for the cells containing the interface (Roenby *et al.*, 2016; Olsson, 2017). The value for the phase fraction in cell i at time t, α_i(t), is calculated from a function H(x; t) describing the continuous phase fraction field:

$$\alpha_i = \frac{1}{V_i} \int_{\Omega_i} H(x,t) dV, \tag{9}$$

where V_i is the volume of cell i and Ω_i represents each cell.

Knowing the phase fraction in each cell at time t, it is desired to calculate the phase fractions at the next time step using the following equation, where the flux of α over each cell face is integrated in time and added together:

$$\alpha_i(t + \Delta t) = \alpha_i(t) - \frac{1}{V_i} \sum_{j \in B_i} s_{ij} \int_t^{t+\Delta t} \int_{F_j} H(x,\tau) u(x,\tau) dS d\tau, \tag{10}$$

where B_i is the list of all faces F_j belonging to cell i, s_{ij} is used to orient the flux to going out from the cell and τ is the variable of integration used in the time step. dS is the differential area vector pointing out of the volume. s_{ij} is either +1 or -1 to ensure that the product $s_{ij}dS$ is always in the direction out form the cell boundary even when the orientation of face j makes dS point into the cell.

3.4 Mesh Refinement and Boundary Conditions.

When a nonparametric mesh is used to represent a cylindrical geometry, the central region of the cylinder assumes a square profile, what would be incompatible with the bubble geometry to be represented in the present work. A possible resource to circumvent this problem is to define arcs internally or externally to that square. On the other hand, the use of a parametric mesh provides other tools able to softening the central region, improving the modeling of curved geometries. Fig.3 presents this two mesh configurations. In the present work, both types of mesh were tested for the simulation of the rise of Taylor bubbles in stagnant water columns.

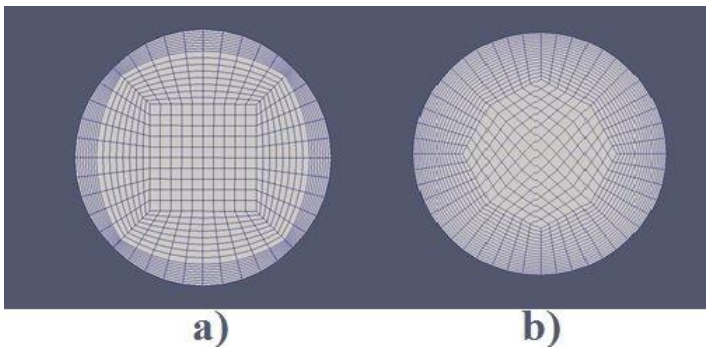

Figure 3. Mesh configurations: a) nonparametric mesh; b) parametric mesh.

Figure 4 represents the phase distribution inside the tube settled as the initial condition of the simulation. The gas phase (red color) was concentrated at the bottom end of the tube in order to represent the air pocket length L_0 described in Fig. 2, after the column rotation. The remainder of the tube was occupied by the liquid phase. The initial velocity of the phases was taken to be zero and the pressure was just the hydrostatic pressure since the simulation was performed for a closed tube.

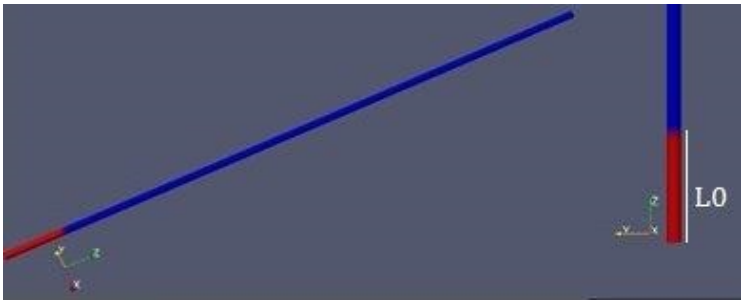

Figure 4. Phase distribution at the initial condition of the simulation.

4. RESULTS AND DISCUSSION

Experiments and computational simulations of single Taylor bubbles rising in a stagnant water column (Figs. 2 and 4) were performed. For simulations, the InterFlow solver with nonparametric and parametric meshes was used.

The Taylor bubble velocities U_0 were determined after the full development of their flows, recovering the bubble axial positions at different time steps of the simulations and calculating the angular coefficients of the best linear fits of these points. An excellent linear fit was observed for all the simulated cases, which confirmed that the rising bubble motion was fully developed, as presented in Fig.5.

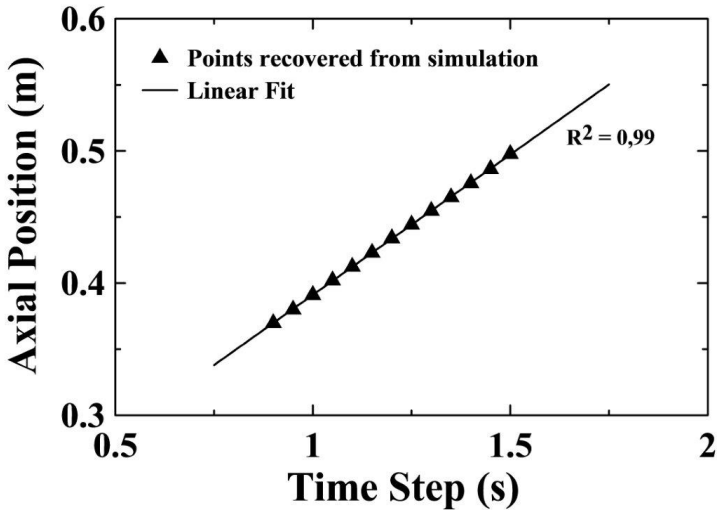

Figure 5. Axial position vs time step relation for a parametric mesh with 116,000 cells.

The data generated by OpenFOAM can be visualized on ParaView software, where several filters allow the extraction of the simulated data. Five filters were used to obtain the simulated bubble profile. The first filter performed the cut of a center plane of the tube (Fig.6a). The second one showed the bubble outline (Fig.6b). The third one marked the points along this outline (Fig.6c). Finally, a fourth filter performed the extraction of the marked points (Fig.6d), and generated a spreadsheet with the coordinates of the extracted points.

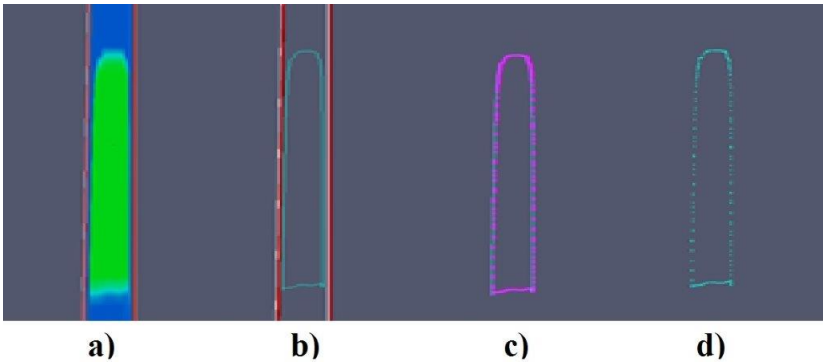

Figure 6. Recovery of the simulated bubble profile.

Initially, simulations were performed using nonparametric meshes with 126,000 cells for bubbles generated from air pocket lengths L_0 of 0.20, 0.30 and 0.40 m, respectively. Fig.7a presents the experimental and the simulated Froude numbers Fr of bubbles generated from different L_0, where $Fr = U_0\sqrt{gD}$. The experimental results presented a very good agreement with the expression proposed by Nicklin *et al.* (1962) to estimate the velocity of an elongated bubble rising in low viscosity liquids. Fig.7a also indicates a disagreement between the simulated and the experimental results. However, the simulated velocities for these bubbles with different lengths were basically the same, which is in agreement with the qualitative behavior observed by Nicklin *et al.* (1962). For Taylor bubbles rising in closed vertical tubes, the bubble rising velocity is independent of the bubble length, which was also observed in the experimental results.

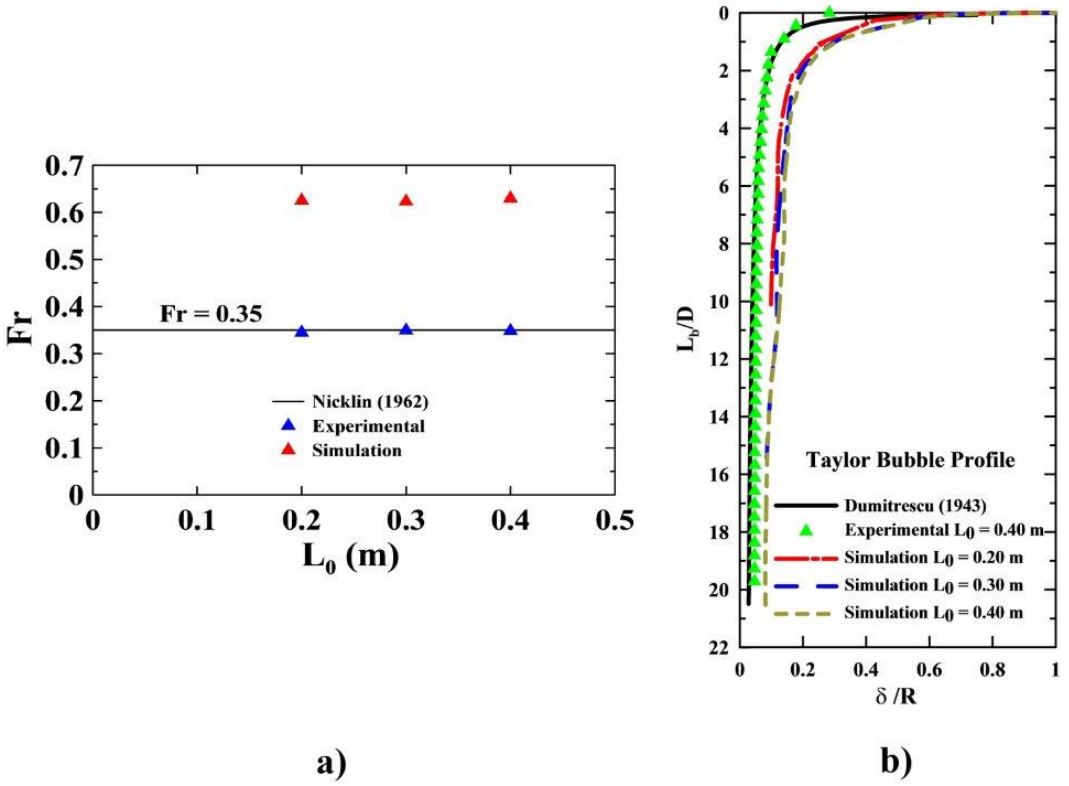

Figure 7. Comparison between the simulated results using nonparametric mesh with 126,000 cells and the experimental ones for bubbles generated from different air pocket lengths L_0: a) Bubble velocities; b) Bubble Profiles.

Figure 7b presents the theoretical (Eqs. (1) and (2)), the experimental and the computational profiles of these single Taylor bubbles. It shows a very good agreement between the experimental measurements and the correlation proposed by Dumitrescu (1943). Despite the slight disagreement observed between the experimental profile and those obtained by computational simulations, one can observe that the simulated bubbles took the typical Taylor bubble profile, which was not achieved in our previous attempts to simulate this type of bubble using the InterFOAM solver. Additionally, it can also be observed a superposition of the profile of bubbles generated from different L_0. This superposition is in agreement with experimental results indicating that an increment on the volume of Taylor bubbles rising in the same experimental conditions (liquid and internal tube diameter) did not change the bubble profile in the nose and film regions (De Azevedo *et al.*, 2017). The bubble growth only occurs from its tail.

A new simulation was performed trying to improve the modeling of the geometry involved in our work, using a parametric mesh with 116,000 cells. This number of cells was settled in order to be close to that used for the simulation with nonparametric mesh (126,000 cells). As would be expected, an improvement was obtained on the computational simulation. Fig.8b shows that the simulated bubble profile presented a very good agreement with the experimental results and, consequently, with the correlation of Dumitrescu (1943). Concerning the bubble velocity, the simulated result still disagreed with the experimental one, as can be observed in Fig. 8a. However, the simulated value obtained by using a parametric mesh was closer to the experimental results than when a nonparametric mesh was used.

Mesh refinement has an important role on computational simulations of Taylor bubbles (or of the slug flow) inside tubes, minitubes or microtubes and the bubble parameters need to be properly captured in order to ensure their appropriate use on applications as the prediction of mass and heat transfer behavior (Zheng *et al.*, 2007; Fletcher and Haynes, 2017). In this way, new simulations were performed using parametric mesh with other mesh refinements: 176,400 and 236,000 cells.

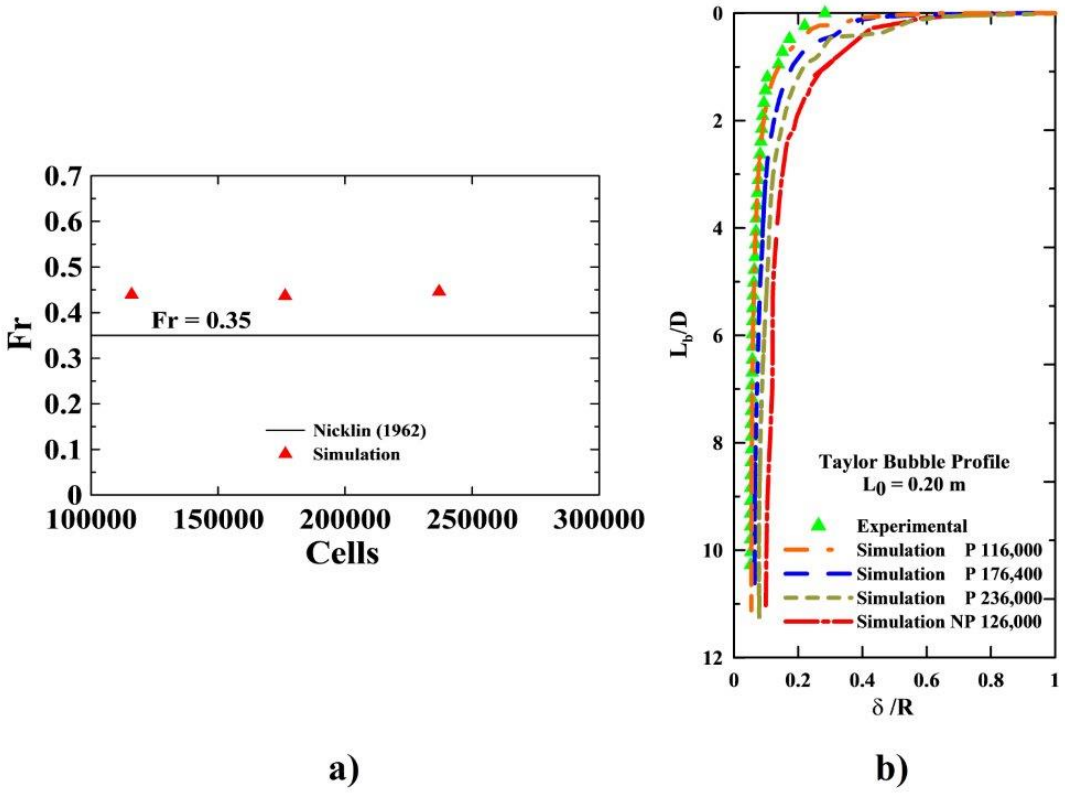

Figure 8. Comparison between the simulated results using parametric (P) mesh with different number of cells and the experimental ones for bubbles generated from $L_0 = 0.20$ m: a) Bubble velocities; b) Bubble Profiles.

Figure 8a shows that the simulated bubble velocities did not change with the increase of the number of parametric cells. However, when the number of parametric cells increased, the bubble profile tended to move away slightly from the experimental profile, especially near to the nose region, as presented in Fig.8b. Simulations were also performed with higher mesh refinements (270,000 and 360,000 cells), however the obtained results presented physical inconsistencies and therefore they were not take into account in the present work.

5. CONCLUSIONS

Computational simulations of single Taylor bubbles rising in a stagnant water column were performed, using the InterFlow solver of the OpenFOAM software with nonparametric and parametric meshes and the results were compared with experimental results and correlations available in the literature.

The simulated bubbles took the characteristic profile of Taylor bubbles and the results obtained using parametric meshes showed to be better than those obtained with nonparametric meshes. For parametric mesh, the different mesh refinements employed did not influence significantly the simulated bubble velocity. On the other hand, the bubble profile moved away slightly from the experimental profile, when the number of cells increased.

Despite the simulated velocities did not presented a good agreement with the experimental results, we consider that the Interflow solver of OpenFOAM seems to be a promising tool for computational simulations of Taylor bubble motion. However, a better knowledge about the Interflow solver is needed in order to perform a more adequate mesh construction and propose modifications to improve the modeling of these bubbles motion, and consequently the simulated results concerning the bubble velocity. As an example, the parametric mesh construction requires the setting of parameters such as the number of cells at the inner square, between the square and the circle and in the cylinder height (Fig.3). The influence of these parameters on the simulated bubble velocity and on the simulated bubble profile needs to be very well understood.

6. ACKNOWLEDGEMENTS

The authors are grateful to CNPq, FINEP, FAPERJ and IEN/CNEN for the financial support.

7. REFERENCES

Davies, R.M. and Taylor, G., 1950. "The mechanics of large bubbles rising through extended liquids and through liquids in tubes". *Proceedings of the Royal Society of London Series a-Mathematical and Physical Sciences*, Vol. 200, No. 1062, pp. 375–390.

De Azevedo, M.B., Dos Santos, D., Faccini, J. and Su, J., 2017. "Experimental study of the falling film of liquid around a taylor bubble". *International Journal of Multiphase Flow*, Vol. 88, pp. 133–141.

Dumitrescu, D.T., 1943. "Stromung an Einer Luftblase im Senkrechten Rohr". *Z. Angew. Muth. Mech.*, Vol. 23, pp. 139–149.

Fletcher, D.F. and Haynes, B.S., 2017. "Cfd simulation of taylor flow: Should the liquid film be captured or not?" *Chemical Engineering Science*, Vol. 167, pp. 334–335.

Ghajar, A.J., 2005. "Non-boiling heat transfer in gas-liquid flow in pipes - a tutorial". *Journal of the Brazilian Society of Mechanical Science and Engeneering*, Vol. 27, No. 1, pp. 46–73.

Hiltunen, K., Jasberg, A., Kallio, S., Karema, H., Kataja, M., Konoppen, A., Manninen, M. and Taivassalo, V., 2009. *Multiphase Flow Dynamics Theory and Numerics*. VTT PUBLICATIONS 722 Edita Prima Oy, Helsinki, 2nd edition.

Hirt, C.W. and Nichols, B.D., 1981. "Volume of fluid (vof) method for the dynamics of free boundaries". *Journal of Computational Physics*, Vol. 39, pp. 201–225.

Nicklin, D., Wilkes, J. and Davidson, J., 1962. "Two-phase flow in vertical tubes". *Trans. Instn. Chem. Engr*, Vol. 40, pp. 61–68.

Nogueira, S., Riethmuller, M.L., Campos, J.B.L.M. and et al, 2006. "Flow in the nose region and annular film around a taylor bubble rising through vertical columns of stagnant and flowing newtonian liquids". *Chemical Engineering Science*, Vol. 61, pp. 845–857.

Olsson, E., 2017. "A description of isoadvector - a numerical method for improved suface sharpness in two-phase flows". In *Proceedings of CFD with OpenSource Software*. Edited by Nilsson, H.

Roenby, J., Bredmose, H. and Jasak, H., 2016. "A computational method for sharp interface advection". *Royal Society Open Science*, Vol. 11, No. 3.

Tryggvason, G., Scardovelli, R. and Zaleski, S., 2011. *Direct Numerical Simulations of Gas-Liquid Multiphase Flows*. Cambridge University Press, Cambridge.

Zheng, D., He, X. and Che, D., 2007. "Cfd simulations of hydrodynamic characteristics in a gas-liquid vertical upward slug flow". *Heat and Mass Transfer*, Vol. 50, No. 21-22, pp. 4151–4165.

8. RESPONSIBILITY NOTICE

The authors are the only responsible for the printed material included in this paper.